



Reynolds number and diffusion coefficient of micro- and nano-aerosols in optical pipelines

Amin Mousavi¹ · Fahimeh Hosseinibalam¹  · Smaeyl Hassanzadeh¹

Received: 15 March 2018 / Accepted: 15 November 2018 / Published online: 20 November 2018
© Springer-Verlag GmbH Germany, part of Springer Nature 2018

Abstract

In this study, the microscopic particle motion inside an optical pipeline, such as particle motion through a mechanical tube, is investigated. The photons in an optical tube guide the particles towards the center of the light beam by inducing photophoretic and radiation pressure forces. Laguerre–Gaussian- and Bessel-like beams are examples of such optical tubes. The Reynolds number of particle motion in optical tubes is investigated. The power of the light beam and the ratio of the particle radius to the light beam ring radius influence the turbulence of the particle flow and the value of the Reynolds number. The diffusion coefficient of particle movement in such pipelines is derived, which indicates that an optical tube is a good tool for guiding and trapping particles in micron- and nanometer-scale dimensions.

1 Introduction

Small particles suspended in gas (aerosols) or liquids (hydrocolloids) start to migrate when illuminated by a sufficiently intense beam of light. Optical inductive forces have introduced a clear pathway for conducting particles in micrometer and smaller dimensions [1–5]. The interaction between electromagnetic waves or photons with matter may involve an exchange of momentum. Due to the law of conservation of momentum, any change in the total momentum of the waves or photons must involve an equal and opposite change in the momentum of the matter it interacted with. This transfer of momentum is the general explanation for what we term *radiation pressure*. This force was first investigated by Ashkin [6]. The *photophoresis* phenomenon arises from the non-uniform distribution of temperature around an illuminated particle in a fluid medium. Moreover, in a fluid mixture of different kinds of particles, migration of various particles may be due to their differences in absorptions of thermal radiation and other thermal effects collectively known as thermophoresis [7]. This phenomenon was first discovered by Ehrenhaft almost 100 years ago [8]. In cone-shaped or doughnut-shaped light beam, both the radiation pressure and photophoretic forces are linearly dependent on

the incoming laser intensity, and guide the light-absorbing particles towards the beam propagation direction and from higher to lower intensity illumination [9–12]. Here, the photons play a similar role as the wall in a mechanical tube by preventing particle diffusion. The movement of microscopic particles in narrow paths in optical tubes is useful for studying particle characteristics. For example, by guiding particles in micrometer dimensions in Bessel rays, the structure of particles was determined using an X-ray Free Electron Laser (FEL) [13]. The radiation pressure is generally much smaller than the photophoretic force when the Knudsen number, $Kn = \frac{\lambda}{R_p}$, is very small ($Kn \ll 1$) [14–18], where λ is the mean free path (average distance traveled between collisions with other gas molecules) of the fluid and R_p is the particle radius.

In this paper, we first analyze the photophoretic force and its influencing factors in Sect. 2.1, and then, we consider the motion of carbon nano-cluster aerosols into LG₀₁ light beam in Sect. 3.1. Velocity, and longitudinal and transverse locations of particles in this tube are investigated. The Reynolds number of particle motion in optical tube is derived in Sect. 3.2 and particle motion turbulence is analyzed. Finally, in Sect. 3.3, the diffusion coefficient of particle motion in optical tube is studied. In this study, Reynolds number and diffusion coefficient of the particle motion in an optical tube are derived for the first time.

✉ Fahimeh Hosseinibalam
fhh@sci.ui.ac.ir

¹ Department of Physics, University of Isfahan,
81746-73441 Isfahan, Iran

2 Trapping and guiding particle droplets in fluxes in an optical tube

2.1 Photophoretic force

Indirect photophoresis occurs as a result of an increase in the kinetic energy of molecules when particles absorb incident light only on the irradiated side, thus creating a temperature gradient within the particle. As a result, the surrounding gas layer reaches temperature equilibrium with the surface of the particle. The molecules with higher kinetic energy in the region of higher gas temperature impinge on the particle with greater momentum compared to the molecules in colder regions, which causes a migration of particles in a direction opposite to the surface temperature gradient [8]. In this paper, we assume an ideal LG₀₁ light beam with the following intensity profile [9]:

$$I(\rho, z) = \frac{P}{\pi} \frac{\rho^2}{w^4(z)} \exp\left(-\frac{\rho^2}{w_1^2(z)}\right), \tag{1}$$

where ρ and z are the radial and axial coordinates, and P is the beam power. In (1), $w(z) = w_1 \sqrt{1 + \frac{z^2}{z_0^2}}$ denotes the ring radius for beam waist w_1 and beam dispersion $z_0 = \frac{2\pi w_1^2}{\lambda}$, where λ is the wavelength of the light beam. To trap particles in this cone-shaped optical tube, aerosols are injected from a nozzle that is perpendicular to the ground, and the LG₀₁ light beam radiates in the opposite direction of the flux flow. Figure 1 shows how particles are trapped by photophoretic force [11]. Figure 1a shows the creation of LG₀₁ light beam. The incident doughnut-shaped beam is radiated upward and focused with a 10× plan achromatize objective lens, and a 4× microscope objective is used to track the particle motion illuminated by white light (WL). The polarization is horizontal, and the offset is in the direction of this polarization.

The large black arrow shows the flow of the particle into the beam, blue arrows are the gravitational and drag forces on the particle, and the red arrows are the optical trapping forces. In Fig. 1b, the measured profile of the doughnut-shaped vortex beam and its cross-sections at various distances from the focal plane are shown, where black arrows illustrate the thermal motion of particles. Figure 1c displays a particle on the z -axis (left) and a particle shifted away from the z -axis (right), and it is observed that the intensity distribution causes the particle to move towards the center of the beam.

For small particles, i.e., $R_p \ll w_1$, the longitudinal and the transverse photophoretic forces, F_z^{PP} and F_ρ^{PP} , can be simplified as follows [10]:

$$F_z^{PP}(z) \cong kP \frac{R_p^4}{2w^4(z)}, \quad F_\rho^{PP}(\rho, z) = -kP \frac{4}{3} \frac{\rho \cdot R_p^3}{w^4(z)}, \tag{2}$$

where the phenomenological coefficient,

$$k = \frac{3\mu_a^2}{l_p \rho_a T(k_p + 2k_a)} \quad \text{for } R_p \ll l_p, \tag{3}$$

has a dimension of inverse velocity. In (3), μ_a denotes the viscosity of the flux, l_p denotes the penetration depth of the beam in the particle, and ρ_p and ρ_a are the particle and flux densities, respectively. T is the temperature in Kelvin, and k_p and k_a are the particle and flux thermal conductivity coefficients. When the particles are about micrometer and smaller, the photophoretic force is much larger than the radiation pressure. At a temperature of 298 K, the photophoretic force exerted by a vortex beam on a spherical carbon nano-cluster with radius $R_p = 1 \mu\text{m}$ is almost 10^4 times greater than the radiation pressure, and it is also greater

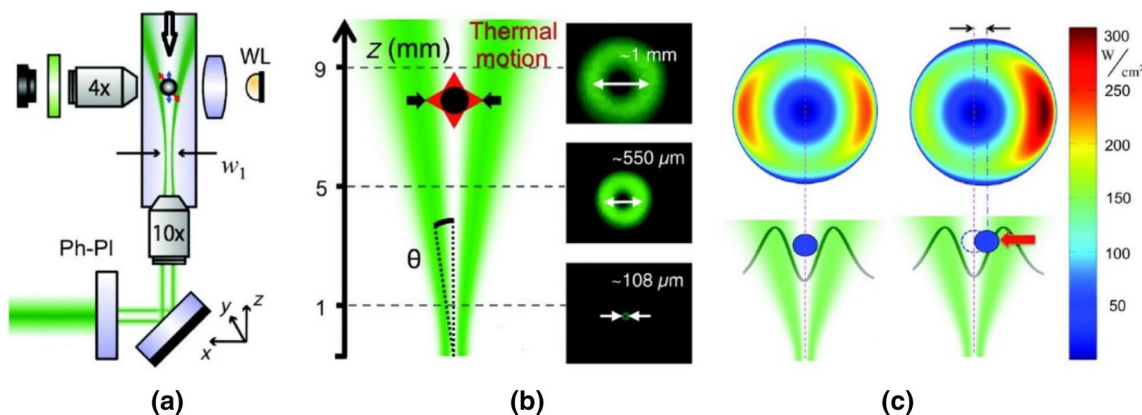


Fig. 1 **a** Using phase plates (Ph-PI), the Laguerre–Gaussian (LG₀₁) light beam is created. **b** The cross-sectional (left) and longitudinal sections (right) of the cone-shaped beam. **c** Trapping particle in the

center of intensity distribution of a LG₀₁ beam because of the non-uniform absorption of photon by particle

than the gravitational force. Therefore, the dominant force in laminar flow is the photophoretic force [9].

2.2 Equations of particle motion in fluxes

According to the Stokes law, the particle motion equation in fluid becomes

$$m_p \frac{dv}{dt} = \frac{3\pi\mu_a R_p}{C_c} (u - v) + \sum_i F_{ei}, \tag{4}$$

$$C_c = 1 + Kn \left[\alpha + \beta \exp\left(\frac{-\gamma}{Kn}\right) \right], \quad m_p = \frac{\pi}{6} R_p^3 (\rho_p - \rho_a), \tag{5}$$

where the first term on the right side of Eq. (4) is the Stokes drag force on a particle moving at velocity v in a flux having velocity u , and F_{ei} denotes the external forces (arising from external potential fields, such as gravity, electrical, thermal and optical forces). In Eqs. (4) and (5), m_p denotes the dynamic mass of the particles in the flux. We note that, C_c , the slip correction coefficient, in air at 1 atm and 298 K for particle with radii 0.01, 0.1, 1, 5 and 10 μm is 22.7, 2.91, 1.168, 1.034 and 1.017, respectively [19–25]. Therefore, the slip correction coefficient becomes more important for nanometer-scale particles, and it is less important for micron particles.

3 Analysis of particle motion in optical tubes

3.1 The trajectory of the particles moving inside the optical tube

According to Fig. 1a, we assume a LG₀₁ laser beam with beam waist $w_1 = 10 \mu\text{m}$ and beam power $P = 100 \text{ mW}$. Carbon nano-cluster particles with radius $R_p = 1 \mu\text{m}$ are injected to the core of the light beam at $z = 2 \text{ cm}$ from the beam waist with a temperature of 298 K. The system parameters of carbon nano-clusters and air are as follows: $\rho_p = 10 \frac{\text{kg}}{\text{m}^3}$, $\mu_a = 1.73 \times 10^{-5} (\text{N} \cdot \text{s})/\text{m}^2$, $\rho_a = 1.29 \frac{\text{kg}}{\text{m}^3}$, $k_a = 0.0262 \frac{\text{W}}{\text{m} \cdot \text{K}}$, $k_p = 0.0266 \frac{\text{W}}{\text{m} \cdot \text{K}}$ and $l_p = 3.5 \times 10^{-5} \text{ m}$ [9]. The particles injected in the beam with an initial longitudinal velocity of $v_z = 50 \text{ m/s}$ and a transverse velocity of $v_\rho = 5 \text{ m/s}$, and the longitudinal and transverse velocity of the flux are also considered the same as longitudinal and transverse velocity of particle. Equation (4) can be separated as follows into the transverse and longitudinal sub-equations based on the direction of flux, and the gravitational and optical forces:

$$m_p \frac{dv_\rho}{dt} = \frac{3\pi\mu_a R_p}{C_c} (u_\rho - v_\rho) + F_\rho^{PP}, \tag{6}$$

$$m_p \frac{dv_z}{dt} = \frac{3\pi\mu_a R_p}{C_c} (u_z - v_z) + F_z^{PP} + m_p g. \tag{7}$$

In Eq. (7), g denotes the gravitational acceleration. Note that Eqs. (6) and (7) are coupled since $F_\rho^{PP}(\rho, z)$ is a function of longitudinal and transverse coordinates, which can be solved using the `x_rkf45` method in the Maple software. Figure 2 shows the transverse position and velocity of the particles with different radii along the longitudinal coordinate and over time, respectively. From Fig. 2a, it can be observed that larger particles move closer to the z -axis, and from Fig. 2b, it is observed that smaller particles are trapped sooner; hence smaller particles are trapped faster.

Figures 3 and 4 display how the light beam power affects the trapping of particles in optical tubes. In Fig. 3, the transverse velocity of a 1- μm carbon nano-cluster particle in an optical tube is shown for various light beam powers, and it is observed that increasing the light beam power results in faster trapping of the particles. Figure 4 shows the transverse position of the particle over time and along the light beam axis z , from which it can be seen that by increasing the beam power the particles are trapped faster and their trajectories are closer to the light beam axis. Higher light beam power implies a larger number of photons, which create a larger temperature gradient. Hence, smaller particles can be trapped in low power beams. The relative ring radius of the optical tube to the particle radius affects the trapping of particles in beams. As observed from Fig. 5, for light beams with smaller waist, the particle trajectory is closer to the beam axis and the particle is trapped faster, while a particle with dimensions larger than the beam waist has a higher chance of escaping the light beam.

3.2 Reynolds number in an optical tube

Transition from laminar to turbulent flow depends on the geometry, surface roughness, flow velocity, surface temperature, and the type of fluid. After exhaustive experiments in the 1880s, Osborne Reynolds discovered that the flow regime depends mainly on the ratio of inertial forces to viscous forces in the fluid. This ratio is called the *Reynolds number*. In flows with large Reynolds numbers, i.e., when inertial forces are much larger than viscous forces, the fluid is *turbulent* since the viscous forces cannot prevent the random and rapid fluctuations of the fluid. However, in fluids with small or moderate Reynolds numbers, the viscous forces are large enough to suppress these fluctuations and to keep the fluid “in line”, resulting in a laminar flow. The Reynolds number of a particle in a fluid is [20]:

$$Re_p = \frac{\rho_a R_p}{\mu_a} (|u - v_\infty|), \tag{8}$$

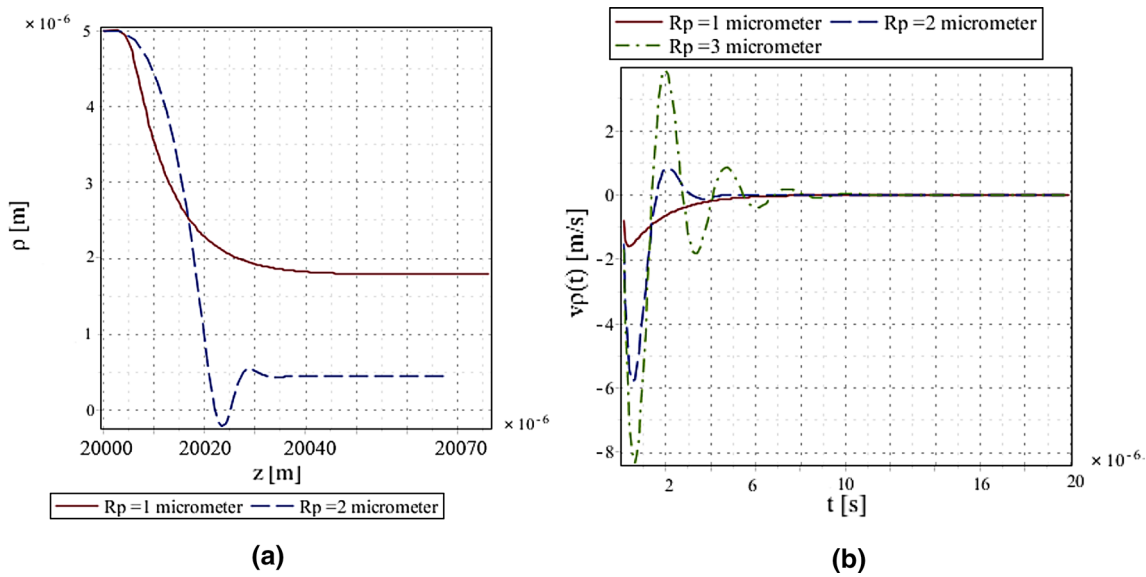


Fig. 2 **a** Transverse position of particles along the light beam axis for particles with radii equal to 1 and 2 μm . **b** Transverse velocity of particles over time for particles with radii equal to 1, 2 and 3 μm

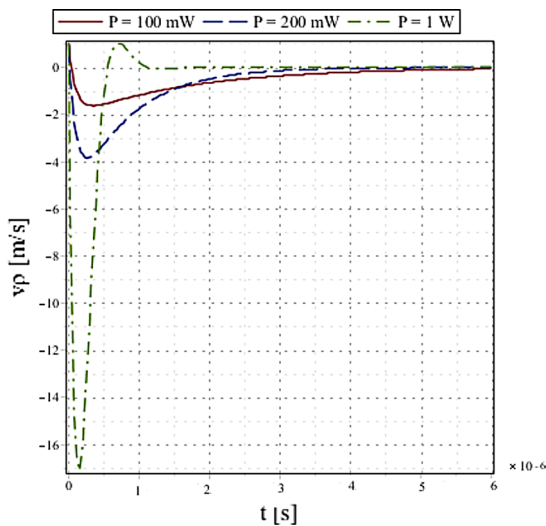


Fig. 3 Transverse velocity of a 1- μm particle over time for different laser beam powers of $P = 100$ mW, $P = 200$ mW and $P = 1$ W

where u is the flux velocity and v_∞ is the certain longitudinal velocity of a particle in the flux, which is obtained by solving Eqs. (6) and (7). Similar to Bessel-like beams, we consider an optical tube with a constant ring radius ($w(z) \sim w_1$). The Reynolds number of particle motion in these light beams is given by

$$Re_p = \frac{\rho_a k P c_c}{\pi \mu_a^2} (\alpha^4), \quad \alpha = \frac{R_p}{w}, \quad (9)$$

which Re_p is a function of fourth power of the particle radii to the beam radius ratio. Figure 6 displays the Reynolds number as a function of this ratio for a light beam with power $P = 100$ mW. For a light beam with a ring radius of 10 μm , nanometer particles, i.e., $R_p < 1 \mu\text{m}$, have less turbulence compared to micron particles.

Even though in optical tube with higher beam powers, particles are trapped much easier, it can make their motion more turbulent and, therefore, result in a higher Reynolds number. Figure 7 illustrates the Reynolds number of carbon nano-cluster particles in light beams with different powers of $P = 10$ mW, $P = 100$ mW and $P = 1$ W. It is observed that in an optical tube, turbulence increases as the beam power increases.

3.3 Particle diffusion coefficient in an optical tube

The movement of particles due to the Brownian motion can be described as a diffusion process. The higher the diffusivity (of one substance with respect to another), the faster they diffuse into each other. The particle diffusion coefficient within a flux is obtained from the following relationship [21–23]:

$$D = \frac{1}{2} \frac{\partial \rho^2}{\partial t}. \quad (10)$$

The diffusion coefficient of particles in an optical tube (solid curve) and without an optical tube (dashed curve) is plotted in Fig. 8. In both cases, the outlet radius of nozzle is 4 μm , and nano-cluster particles move in an optical tube

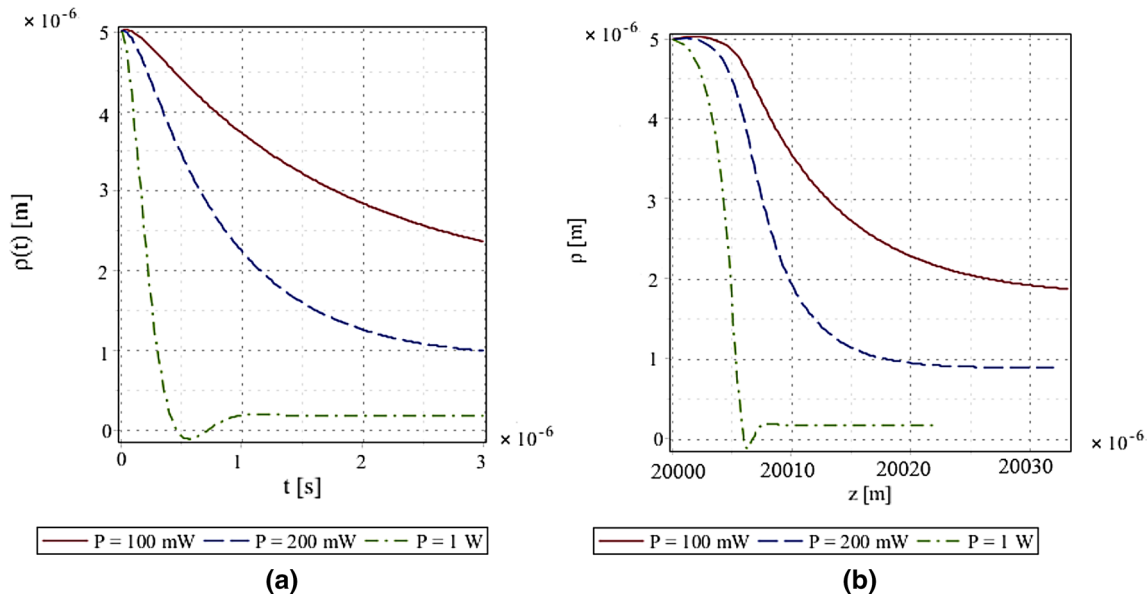


Fig. 4 Transverse position of a 1- μm particle for LG_{01} beam powers of $P = 100 \text{ mW}$, 200 mW and 1 W **a** as a function of time, **b** along the light beam axis z

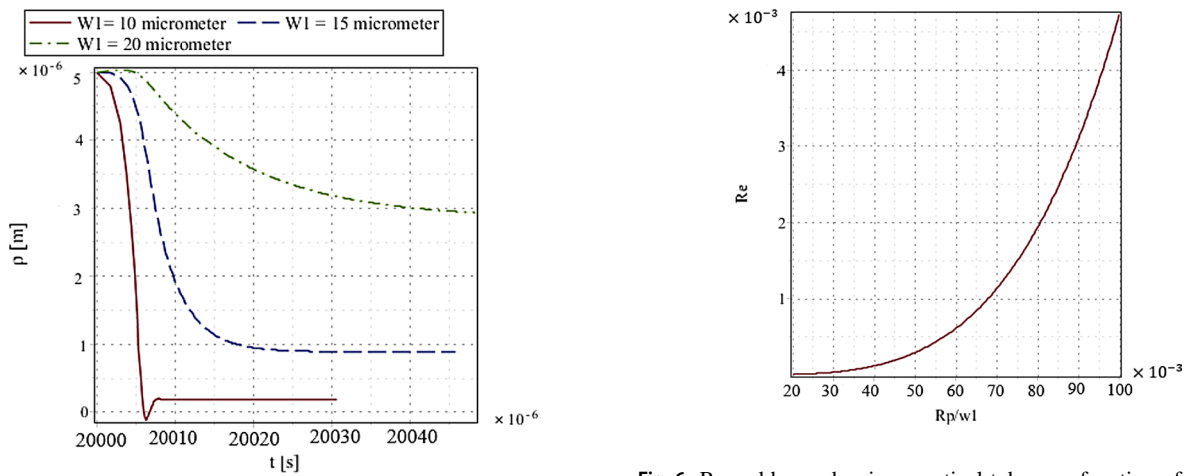


Fig. 5 Transverse position of a 1- μm particle over time for different laser beam waists of $w_1 = 10 \mu\text{m}$, $w_1 = 15 \mu\text{m}$ and $w_1 = 20 \mu\text{m}$.

Fig. 6 Reynolds number in an optical tube as a function of the particle radius to the beam waist ratio for beam power $P = 100 \text{ mW}$

with $P = 100 \text{ mW}$ and $w \sim w_1 = 10 \mu\text{m}$. The characteristics of this flux are similar to that in Sect. 3.1. According to Fig. 8, the diffusion coefficient of nanometer and micron particles without an optical tube is not significantly different for different particles. If an optical tube is used for guiding the particles, the diffusion coefficient of the larger particles decreases on a micron scale because, according to Fig. 2a, larger particles are trapped closer to the light beam axis. In general, the presence of an optical tube reduces the particle diffusion coefficient. The diffusion coefficient depends on the location of the particles around the axis of the beam. Therefore, it can be concluded that factors such

as beam power and light beam waist affect the particle diffusion coefficient in the same way.

4 Conclusion

Particles can be guided in a pipe-like manner in a flux using cone-shaped light beams, such as LG_{01} or Bessel-like beams. Therefore, such tubes are also called optical tubes. Guiding particles inside optical tubes is significantly different from guiding them in mechanical tubes. When $Kn \ll 1$, the dominant optical force on particles in a fluid is the photophoretic force. When guiding micrometer aerosols into a LG_{01} beam, smaller particles are trapped into

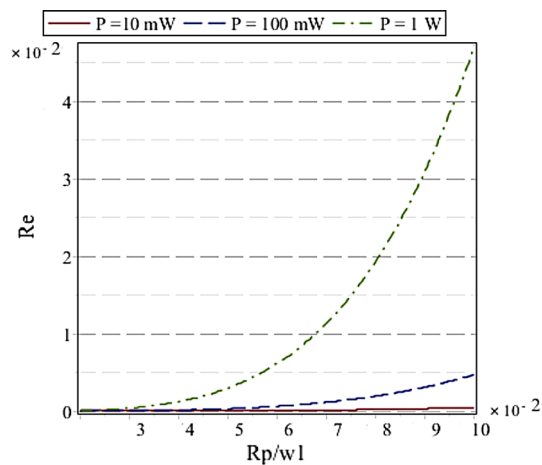


Fig. 7 Reynolds number in an optical tube as a function of the particle radius to the beam waist ratio for different beam powers of $P=10$ mW, $P=100$ mW and $P=1$ W

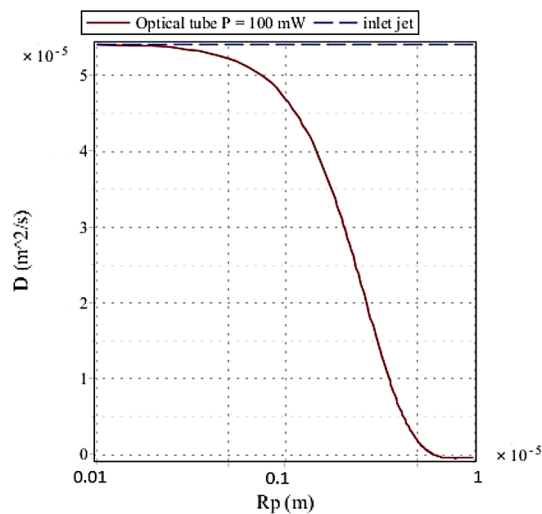


Fig. 8 The diffusion coefficient for particles are injected from an inlet jet in the air according to Fig. 1a (blue dashed curve) and for particles injected in an optical tube (red solid curve), versus particle radius (R_p)

the tube faster and larger particles are trapped closer to the light beam axis. With a small displacement in the optical tube, the particles travel to the beam axis at a certain longitudinal velocity. The light beam power plays an important role in guiding and trapping the particles in paths that are parallel to the beam axis. These paths become closer to the beam axis as the beam power increases. Particles are trapped slower in light beam with larger radius. In a light beam with a constant radius, the Reynolds number of the particles motion is highly dependent on the particle radius to light beam radius ratio, and for larger particles the diffusion is less. The light beam power also affects the

turbulence of particles inside optical tubes. Based on our results that the diffusion coefficient for particles is much lower in optical tubes, optical tubes are a good candidate for using in optical methods when studying microscopic particles.

References

1. D. McGloin, D.R. Burnham, M.D. Summers, D. Rudd, N. Dewar, S. Anand, Optical manipulation of airborne particles: techniques and applications. *Faraday Discuss.* **137**, 335–350 (2008)
2. D.R. Burnham, D. McGloin, Modeling of optical traps for aerosols. *JOSA B* **28**, 2856–2864 (2011)
3. V.G. Shvedov, A.V. Rode, Y.V. Izdebskaya, A.S. Desyatnikov, W. Krolikowski, Y.S. Kivshar, Giant optical manipulation. *Phys. Rev. Lett.* **105**, 118103 (2010)
4. Z. Zhang, D. Cannan, J. Liu, P. Zhang, D.N. Christodoulides, Z. Chen, Observation of trapping and transporting air-borne absorbing particles with a single optical beam. *Opt. Express* **20**, 16212–16217 (2012)
5. O. Schmidt, M. Garbos, T. Euser, P.S.J. Russell, Metrology of laser-guided particles in air-filled hollow-core photonic crystal fiber. *Opt. Lett.* **37**, 91–93 (2012)
6. A. Ashkin, Acceleration and trapping of particles by radiation pressure. *Phys. Rev. Lett.* **24**, 156 (1970)
7. Sh. Tehrani, Photophoresis of micrometer-sized particles in the free-molecular regime. *Int J Heat Mass Transf.* **44**, 1649 (2001)
8. F. Ehrenhaft, On the physics of millionths of centimeters. *Phys. Z* **18**, 352–368 (1917)
9. A.S. Desyatnikov, V.G. Shvedov, A.V. Rode, W. Krolikowski, Y.S. Kivshar, Photophoretic manipulation of absorbing aerosol particles with vortex beams: theory versus experiment. *Opt. Express* **17**, 8201–8211 (2009)
10. M. Summers, J. Reid, D. McGloin, Optical guiding of aerosol droplets. *Opt. express* **14**, 6373–6380 (2006)
11. N. Eckerskorn, R. Bowman, R.A. Kirian, S. Awel, M. Wiedorn, J. Küpper, M.J. Padgett, H.N. Chapman, A. Rode, Optically induced forces imposed in an optical funnel on a stream of particles in air or vacuum. *Phys. Rev. Appl.* **4**, 064001 (2015)
12. J.A. Rodrigo, A.M. Caravaca-Aguirre, T. Alieva, G. Cristóbal, M.L. Calvo, Microparticle movements in optical funnels and pods. *Opt. Express* **19**, 5232–5243 (2011)
13. N. Eckerskorn, L. Li, R.A. Kirian, J. Küpper, D.P. DePonte, W. Krolikowski, W.M. Lee, H.N. Chapman, A.V. Rode, Hollow Bessel-like beam as an optical guide for a stream of microscopic particles. *Opt. Express* **21**, 30492–30499 (2013)
14. E.J. Davis, G. Schweiger, in “The airborne microparticle: its physics, chemistry, optics, and transport phenomena”, ed. by S.S.B. Media (Springer, Berlin, 2002), pp. 755–810
15. S. Beresnev, V. Chernyak, G. Fomyagin, Photophoresis of a spherical particle in a rarefied gas. *Phys. Fluid A Fluid Dyn* **5**, 2043–2052 (1993) (1989–1993)
16. A. Melzer, Laser manipulation of particles in dusty plasmas. *Plasma Source. Sci. Technol.* **10**, 303 (2001)
17. H.C. Weng, On the importance of thermal creep in natural convective gas micro flow with wall heat fluxes. *J. Phys. D Appl. Phys.* **41**, 115501 (2008)
18. YU. I. Yalamov, V. B. Kutukov, and E. R. Shchukin, Theory of the photophoretic motion of the large-size volatile aerosol particle. *J. Colloid Interface Sci.* **57**, 564–571 (1976)

19. F.F. Abraham, A.C. Zettlemoyer, Homogeneous nucleation theory. *Phys. Today* **27**, 12–52 (1974)
20. M.K. Alam, The effect of van der waals and viscous forces on aerosol coagulation. *Aerosol. Sci. Technol.* **6**, 41–52 (1987)
21. M.D. Allen, O.G. Raabe, Re-evaluation of Millikan's oil drop data for the motion of small particles in air. *J. Aerosol. Sci.* **13**, 537–547 (1982)
22. R.B. Bird, W.E. Stewart, E.N. Lightfoot, *Transport Phenomena* (Wiley, Amsterdam, 1960)
23. B.V. Derjaguian, Y.I. Yalamov, *The Theory of Thermophoresis and Diffusiophoresis of Aerosol Particles and Their Experimental Testing* (Pergamon Press, Oxford, 1972)